Sains Malaysiana 51(10)(2022): 3423-3436
http://doi.org/10.17576/jsm-2022-5110-25

A Geant4 Simulation on the Application of Multi-layer Graphene as a Detector Material in High-energy Physics

(Simulasi Geant4 ke atas Pengaplikasian Grafin Berbilang Lapisan sebagai Bahan Pengesan dalam Fizik Bertenaga Tinggi)

NURUL HIDAYAH MOHAMAD NOR[1,2,*], NUR AFIRA ANUAR[2], WAN AHMAD TAJUDDIN WAN ABDULLAH[1], BOON TONG GOH[2] & MOHD FAKHARUL ZAMAN RAJA YAHYA[3]

[1]National Centre for Particle Physics, Universiti Malaya, 50603 Kuala Lumpur, Federal Territory, Malaysia
[2]Low Dimensional Material Research Centre, Department of Physics, Faculty of Science, Universiti Malaya, 50603 Kuala Lumpur, Federal Territory, Malaysia
[3]Faculty of Applied Science, Universiti Teknologi MARA, 40450 Shah Alam, Selangor Darul Ehsan, Malaysia

Received: 3 Jan 2022/Accepted: 25 May 2022

ABSTRACT

The excellent properties of graphene, such as its high thermal conductivity, high electrical conductivity, and high electron density, make it an ideal candidate as a detector material in high-energy physics applications. In this work, we demonstrate the feasibility of multi-layer graphene (MLG) as a detector material in a high-energy environment. The Geant4 software package was used to estimate the energy of the deposited electrons within various thicknesses of MLG, ranging from 3 to 20 nm. The efficiency of the MLG as a detector material was further analyzed from the scattering angle and the yield of the secondary particles produced from the electron interaction with the material. The incident electron's kinetic energy used herein ranged between 30 keV and 1 GeV, at a particle fluence of 1×10^7 e/cm^2. The results show that the deposited energy was relatively low for the interaction with 1 MeV electrons, and dramatically increased as the thickness increases beyond 15 nm. This result was further supported by the highest yield of gamma radiation recorded by the interaction with a kinetic energy larger than 1 MeV, for thickness larger than 15 nm. The results suggest that the MLG works best as a charged particle detector in low energy ranges, while for high energy ranges, a thickness over 15 nm is suggested. The findings demonstrate that a MLG with a thickness larger than 15 nm could potentially be used as a detector material in high-energy conditions.

Keywords: Detector material; Geant4; Monte Carlo simulation method

ABSTRAK

Ciri cemerlang grafin seperti kekonduksian terma, kekonduksian elektrik dan ketumpatan elektron yang tinggi telah menjadikannya calon yang ideal sebagai bahan pengesan dalam aplikasi fizik bertenaga tinggi. Kajian ini menunjukkan kebolehlaksanaan grafin berbilang lapisan (MLG) sebagai bahan pengesan dalam persekitaran bertenaga tinggi. Perisian Geant4 digunakan untuk mengukur tenaga elektron terdeposit dalam pelbagai ketebalan MLG, antara 3 hingga 20 nm. Kecekapan MLG sebagai bahan pengesan dianalisis selanjutnya dari sudut serakan dan hasil zarah sekunder yang dihasilkan daripada interaksi elektron dengan bahan. Tenaga kinetik elektron yang digunakan di sini adalah antara 30 keV hingga 1 GeV, pada kelancaran zarah 1×10^7 e/cm^2. Hasil kajian menunjukkan bahawa tenaga yang didepositkan adalah agak rendah untuk interaksi dengan elektron 1 MeV dan bertambah baik secara mendadak dengan ketebalan melebihi 15 nm. Keputusan ini disokong lagi oleh hasil sinaran gamma tertinggi yang diperoleh untuk interaksi dengan tenaga kinetik lebih besar daripada 1 MeV bagi ketebalan melebihi 15 nm. Hasil kajian ini menunjukkan bahawa MLG berfungsi paling baik sebagai pengesan zarah bercas dalam julat tenaga rendah, manakala untuk julat tenaga tinggi, ketebalan melebihi 15 nm dicadangkan.

Kata kunci: Bahan pengesan; Geant4; kaedah simulasi Monte Carlo

Introduction

Graphene has outstanding properties, such as its electrical, mechanical, and optical aspects (Castro Neto et al. 2009; Jeong et al. 2012; Nur Afira et al. 2021). This single atomic layer of the carbon allotrope, bonded in a hexagonal lattice (Meyer et al. 2008), is the fundamental component of the carbon-based nanomaterial, such as for carbon nanotubes (CNTs), fullerenes, and Graphite. The electrical conductivity changes in graphene can be easily achieved by modifying its structure and doping, which enables applications in various sensors and detectors (Kholili 2015; Liu et al. 2011). In addition to that, this thinnest and strongest ever known material also showed promising potential for miniaturization of electronic components. Its good thermal conductivity, high electron density (Moser et al. 2007), and high electron mobility, making graphene an ideal candidate for detector materials in high-energy physics (HEP) applications, where radiation hardness and superfast responses are crucial (Bortoletto 2015; Metcalfe et al. 2014; Schmidt 2016) for high-performance detectors. Graphene has been reported to work best with high cut-off frequencies (1 GHz), proving that it has the ability to produce a swift response (Lin et al. 2009) during detection in high-energy experiments. The ideal graphene is usually visualized as a perfectly flat two-dimensional material, with high electronic conductivity due to the low defect density of its crystal lattice (Singh et al. 2011). Its good conductivity properties, which is ideal as a detector material, has been commonly reported in high-quality single and bilayer graphene. However, the small interaction medium, notably in single and bilayer graphene, may cause the loss of signal generation in the medium itself. The high-energy particle may only be transmitted in the thin film medium without generating any detectable signal (Banhart 1999; Compagnini et al. 2009; Krasheninnikov & Banhart 2007). This effect will deteriorate the efficiency of the detector, which is not favorable in this application. Despite its good conductivity, the thickness of the interaction medium also plays a vital role in detector design, specifically in a high-energy environment (Kholili 2015).

Multilayer graphene (MLG) which has a typical thickness ranging from 5 nm to 200 nm, as reported by Murata et al. (2019), has the advantages over single-layer graphene in terms of its medium interaction thickness. The MLG has been reported to have an excellent electrical and thermal conductivity, with a current-carrying capacity exceeding that of metal (Cu) (Balandin 2011; Biswas & Drzal 2010; Murata et al. 2019). A high electrical conductivity (>2000 S/cm) was achieved for MLG thicknesses between 10 - 100 nm, as reported by Murata et al. (2019). Nur Afira et al. (2021) also reported an increase in the conductivity of the multi-layer graphene (MLG) samples, as compared to the single or bilayer graphene grown via Hot Wire Chemical Vapor Deposition (HWCVD) methods, in a controlled argon (Ar) plasma treatment environment. This excellent MLG property will further enable the exploration studies on the applicability of this carbon material's family for detector applications. The Monte Carlo method has been widely used to simulate HEP interactions with matter due to its ability to model very complex systems using random events (Buckley et al. 2019). This method uses random sampling to predict the probability and uncertainty in a possible interaction. Apart from reducing waste and complicated working procedures, using physical experiments, the Monte Carlo method can also factor in a wide range of parameters and inputs by considering all possible processes and randomness in the process itself. Due to its random nature, this method is much more probabilistic in describing the nature of the interactions between materials and incident particles. Several Monte Carlo tools and codes have been developed for modelling the particle's transport in the matter, such as Geant4, PENELOPE, MCNP, and FLUKA (Guatelli et al. 2011). Amongst the list, Geant4 has been intensively used in particle detector simulation for complex and large-scale HEP experiments, such as in LHC and COMET experiments. This object-oriented toolkit simulates the particle's passage through the matter (Carrier et al. 2004), and traces the incident and secondary particles as they interact with the different materials according to the implemented physics models. In this simulation study, Geant4 has several advantages over other codes, as it includes complete functionality ranges, including tracking, geometry, physics models, and hits. The physics process in the Geant4 is also comprehensive, as it includes electromagnetic and hadronic processes, with a large set of particles, materials, and elements, for a wide range of energies, starting from 250 eV to TeV.

Although graphene has been studied in various detector applications such as for gas detectors (Kim et al. 2008; Lu et al. 2009), chemical detectors (Ang et al. 2008; Zhang et al. 2010), and biomolecular detectors (Robinson et al. 2008; Schedin et al. 2007), its application in HEP experiments is still rarely reported. Notably, in the HEP experiment, the detectors experience the most significant radiation damage from the high luminosity resulting from the particle's collision. Thus, further

studies on the working range, signal generation, detection mechanism, and radiation tolerance of graphene as a potential detector material with the various incoming incidents angles is of great interest. The objective of this study was to evaluate the potential of thin-films Graphite and multi-layer graphene as detector materials under high-energy irradiation.

In the first part of this paper, the Monte Carlo based Geant4 code was used to study the feasibility of the carbon family materials, i.e., thin-films Graphite, and the widely used detection material in HEP, i.e., Silicon (Si), as a detector material in high-energy irradiation. Both materials were analyzed based on the required properties for detection performance. Based on the best detection performance and radiation tolerance of the thin-films Graphite compared to that of Si, further studies were carried out on the MLG using the Geant4 software. This study was driven by the impressive properties of graphene pertaining to its electrical and thermal conductivity, and the outstanding mechanical properties reported in the previous studies (Lee et al. 2008; Mayorov et al. 2011; Moser et al. 2007). The detection performance of different thickness MLGs with the incident electron energies varied from 30 keV – 1 GeV, and was further explored and discussed using the performance parameters, i.e., the deposition energy, scattering angle, and yield of the secondary particles.

MODELLING PROCEDURE

The Geant4 Monte Carlo (version 10.4-patch version 2) simulation was used to investigate the performance of Si, thin-films Graphite, and MLGs as detection materials in this study. The physical hardware used for the Monte Carlo simulation is Personal computer (PC) with single 3.4 GHZ CPU processor and 7.7 GBytes of physical memory, using uBuntu 18.04.3 LTS as operating system. The Physics model selected for the simulation covered the interaction energy in the range of 250 eV up to 1 GeV. The energy of mono-energetic electron that was used as the beam source in each run was set in PrimaryGeneratorAction class. Each run contained n = 1×10^7 number of events. The flow chart for building the simulation in the Geant4 is shown in Figure 1(a). For the first part of the study, Si and thin-films Graphite with thicknesses between 50 µm, 150 µm, 300 µm and 500 µm, were used as absorber materials. On the other hand, the MLG was used as the absorber material for the second part of the study, with the thickness referred to as the number of graphene layers. The density and atomic number used for both Si and thin-films Graphite were as follows: Si 2.330 g/cm^3, z=14; Graphite 2.26 g/cm^3, z=6. The performance of both materials was studied and compared using energy deposition, energy resolution, and detection efficiency at a 1 MeV electron incident energy setting. The 1 MeV electron beam was set parallel to the absorber material at a 2 cm × 2 cm dimension, with the thickness varying from 50 – 300 µm. The density and atomic number used for MLG is 1.7 g/cm^3 and z=6. Each sample was repeated with the incident energy being varied from medium (30 keV- 500 keV), to a high energy range (1 MeV - 1 GeV). Figure 1(b) shows the representative schematic diagram of the simulation setup for both parts of the study. Each Monte Carlo simulation takes on average 2 h of CPU time to be completed.

Energy loss by the charged particles travelling inside the material with a specific energy was computed using the Bethe Bloch formula in the Geant4. Two main processes contributing to the energy loss of charged particles were the ionization process, and the Bremsstrahlung process (Holbert 2012) Geant4 imposed a limit on the step size of the particles and computed the energy loss during the step travelled by the particles. The computational mean of the energy loss during the step used the Bethe-Bloch formula and inverse range of the materials. Since the mass of an electron is inherently small, the Bethe-Bloch formula for the relativistic correction was used instead of its rest mass. This corrected version considered the indistinguishable properties for the identical electrons during the collision. It is crucial to consider this factor to be able to calculate the maximum transferable energy, since electrons experience large deflection from the collisions due to their small mass (Meroli 2015).

The detection efficiency presented in this study corresponded to the material's ability to detect incoming particles. It was calculated using the percentage of particles detected over the emitted particles (Le Bleis & Klenze 2014). Particles which deposited energy values larger than the ionization energy of the graphene were used in the efficiency calculation, ε_D (Hossain et al. 2012). The electron-hole generation calculated from the total energy deposition was divided by the ionization energy of the material (Moll 2006). In order to study the ability of the detector material to interact with the energy of the incoming electron irradiation effectively, the energy resolution was calculated from the full width at half maximum (FWHM) of the energy distribution deposited in graphene, following the irradiation:

$$\mathrm{FWHM} \approx 2.35\,\sigma \qquad (1)$$

$$R = \frac{FWHM}{E_0} \times 100 \quad (2)$$

where σ is the standard deviation; R is the energy resolution; and E_0 is the incident energy (Demir & Kuluöztürk 2021).

The geometry and output results were visualized using the OpenGL in the Geant4. Histograms from the output data were generated using ROOT. Data obtained from the simulation was analyzed and plotted to study the graphene structure and incident energy's effect on the deposited energy, its scattering angles, and detection efficiency.

The Pearson correlation coefficient test was performed to determine the strength of the association between the deposited energy and scattering angles in the MLG, whereby, R=1 was considered as perfect positive relationship between both the variables.

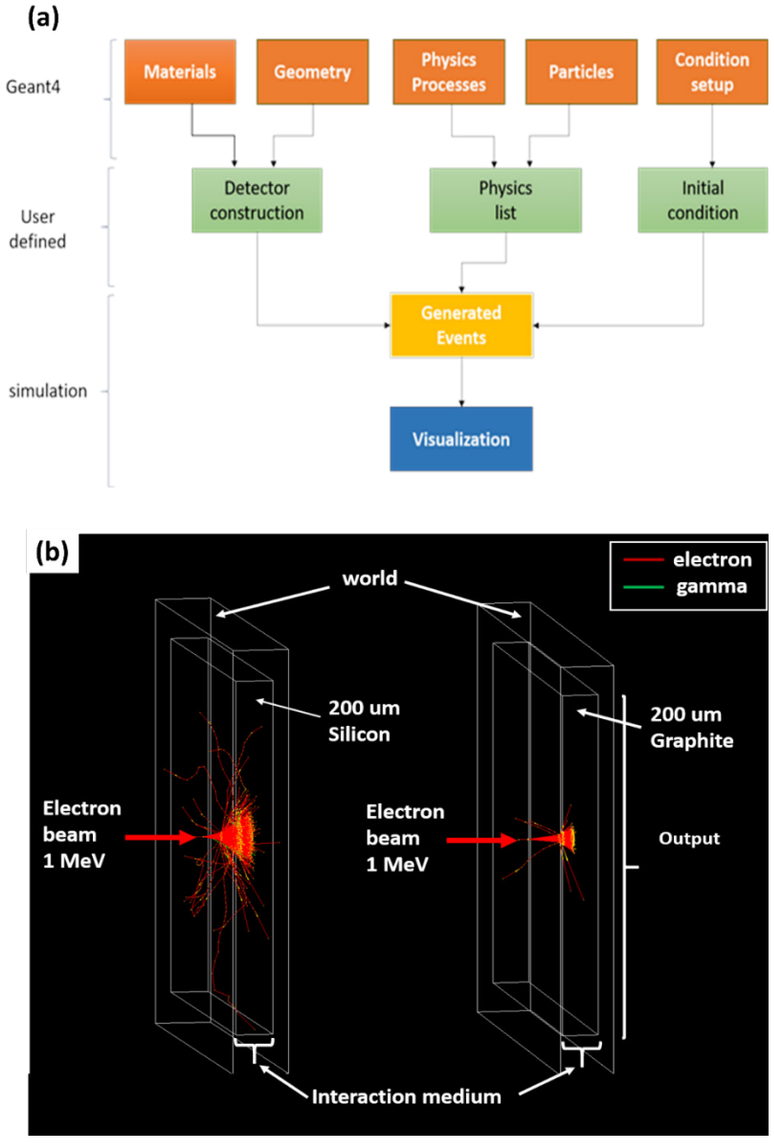

FIGURE 1. (a) Representative flow chart of simulation in Geant4 (b) The cross-section image of 200 μm Si and thin-films Graphite during interaction with 1 MeV electron beam as simulated in Geant4 (n= 10,000). Electrons are visible as red tracks, while green represents gamma

Results & Discussion

Comparison between Silicon and Thin-Films Graphite as Detector Materials in High-Energy Environments

Energy Deposition Analysis

The distribution of the deposited energy across the 50 µm, 150 µm, 300 µm, and 500 µm thicknesses of Si and thin-films Graphite are shown in Figure 2(a) - 2(d). The deposited energy was used to study the most probable energy loss from the incident electron in the material, which is essential for particle identification and signal generation in detectors. All the energy distributions followed the Landau-Vavilov distribution for thin-films as previously reported by Lechner (2018) and Meroli (2015) for interaction with Si thin-films. It was observed that the peak skewed with a long-tail being formed towards a higher energy range, due to the emission of the Bremsstrahlung photons/gamma from the radiative losses, which traveled much further than the electrons. The distribution nearly followed the Gaussian distribution for thicker interaction mediums, as shown for samples with thicknesses of $t \geq 300$ µm (Meroli 2015). It can be seen from the graph that the mean deposited energy was higher in Si compared to thin-film Graphite for all the sample thicknesses, which resulted from the higher density of Si. This result was from the significant scattering in Si compared to thin-films Graphite during the interaction with the high-energy electrons. The higher atomic number (Si: 14, Graphite: 6) and lower radiation length (Si: 9.37 cm, Graphite: 19.32 cm) of Si was attributed to the numbers of electrons scattering within the medium, and resulted in the broadening of the scattering angle at the exit point. In their study, Kumar et al. (2018) reported that the scattering angle of electrons was associated with the fractional radiation length and the atomic numbers of the material used in the interaction medium. The minimal scattering angle observed in thin-films Graphite suggests that a lower budget cost would be incurred in terms of the material required for its implementation in the detector's construction. This low material budget is crucial, especially in HEP experiments, due to the limited space available within the detection area, and to reduce the support structure required for additional maintenance, as a result of exposure to the high radiation environment (Bachmair 2016). This will not only add more cost and space, but also increase the unwanted scattering effect inside the detection cavern (Schmidt 2016). Despite large-signal generation in the medium, these effects will also result in the loss of incident electron energy, reducing the precision and sensitivity of the detection material. An accurate measurement of the particle trajectories is essential, especially in momentum calculation for particle identification of secondary vertices in HEP (Bachmair 2016).

Energy Resolution

To further investigate the performance of Si and thin-films Graphite as detection materials in a high-energy radiation environment, the energy resolution for both materials was calculated from the full width at half maximum (FWHM) of deposited energy peak as a function of material's thickness. Figure 2(e) depicts the energy resolution of both Si and thin-films Graphite for all the samples thicknesses calculated from the fitted energy deposition distribution using the Gaussian curve. This analysis provided important information on the material's sensitivity for particle identification in detector applications (Le Bleis & Klenze 2014; Hossain et al. 2012). All the samples showed an increasing trend for the FWHM, with the increment in the thickness. The higher energy resolution as a result of significant broadening of the FWHM in Si, as compared to the thin-films Graphite with the same thickness, indicated its lower sensitivity in distinguishing between different peaks for detection purposes (Le Bleis & Klenze 2014). Hossain et al. (2012) reported that the larger FWHM of the sodium iodide detector compared to the high purity germanium detector indicated that the material had a lower sensitivity, and that it could be used for detectors that contributed to low energy resolutions. The large scattering properties were speculated to have transpired from this reduction of the energy resolution in the Si. Thus, thin-films Graphite showed better energy resolution for detection, regardless of the thickness. This property is believed to be beneficial for application in high luminosity HEP experiments, where pile-up due to the large event rates produces unwanted signals, and confuse the tracking detectors (Schmidt 2016). The ability of Graphite to detect smaller energy differences is expected to result in less occupancy in the interaction medium, which makes it a suitable material for application in a high luminosity environment.

Detection Efficiency and Signal Generation

Next, the capability of Si and thin-films Graphite as detector materials can be further analyzed from the detection efficiency, ε_D. Figure 2(f) shows the detection efficiency, ε_D calculated from the percentage ratio of the ionized electrons over the total incident electron.

The ionizing energy is defined as the minimum energy required to produce electron-hole pairs, which also involves the excitation of the lattice vibrations, whereby, the value is larger than the minimum ionizing particle (MIP) of the material (Spieler 2005). The ε_D for both samples reduced with the material's thickness, with a more notable reduction being observed for Si samples. The significant reduction in the ε_D of the Si was between ~3% and 12% as compared to thin-films Graphite, with only ~ 0.5 % and ~1% for thicknesses of 300 μm and 500 μm, respectively. This implied that the effects of backscattering and reflected electrons from the interaction were much more dominant in Si due to the high Z number. Razaghi et al. (2019) reported that the detection efficiency of Pb decreased with the thickness and saturation after the optimum thickness of 40 layers.

In contrast to high deposited energy reported in the thicker mediums, as discussed in the section before, the ε_D depends on the signal generation per electrons, and is much more reliable in representing detection efficiencies in the medium. Besides the number of electrons detected in the medium, ionization energy also plays an important role in signal generation. The electron-hole pairs generation for thin-films Graphite was lower than Si with the same thickness, which was due to the lower ionization energy of Graphite (3.96 eV), compared to silicon (3.87eV) (Grupen et al. 2008). A significant difference in the signal generation was more profound for the interaction medium thicker than 150 μm between both samples. Instead of signal creation from the electron-hole pair generation, the intrinsic noise may also affect the signal generation in the material. The intrinsic noise in Graphite was low due to the semi-metal properties, which required only ohmic contact for conductivity purposes.

As for Si, a p-n junction must be created for conducting current and operating under the reverse biased condition to reduce the intrinsic noise. This operating condition not only affects the reduction in the carrier's concentration of Si, but also reduces the signal-to-noise ratio, which is not favorable in detector applications (Kumar et al. 2018). Kumar et al. (2018) also reported that a higher number of e-h pairs were generated in Si (≈23220 electrons), compared to diamond (≈9826 electrons) for a 300 μm thickness. However, this resulted in contra to signal to noise ratio, which showed a lower value in Si (≈41.9), than in diamond (≈57.1). The high intrinsic noise concentration in Si was possibly from the leakage current at the p-n junction, or possibly originated from the defects created during the growth of the silicon. The amplification of the signal can increase the signal-to-noise ratio of Graphite by enhancing the internal gain. However, a more complex architecture is required to increase the signal-to-noise ratio in silicon.

Thin-films graphite has shown better sensitivity and efficiency from the energy resolution, and signal generation studies with a high-energy electron beam (1 MeV), versus Si, as reported in this section. By decreasing the thickness t<150 μm, the energy resolution and $_D$ were much more improved in thin-films Graphite, which gave a good insight into the further application of thinner materials for detector applications. Thin-films graphite exhibited few limitations in signal generation and carrier separation for device applications, despite high sensitivity and efficiencies due to its conductor properties. Further studies on electron beam interactions with thinner carbon-based materials such as graphene may lead to a better signal generation due to lower ionization energies, with an equivalent detection performance. In addition, graphene offers more advantages, such as better conductivity and flexible material properties, which have become more crucial in the developments of future tracking detectors (Hartmann & Kaminski 2011; Schmidt 2016). Graphene layers, especially in MLG, reduce the scattering during electron beam irradiation, and result in a more negligible energy loss probability in the medium (Girit et al. 2009; Wang et al. 2020). Wang et al. (2020) reported that few graphene layers with thicknesses between two to six layers were more prone to defects created by the irradiation due to the weak bonding with a small number of layers. A high-energy electron beam of 1 MeV is required to create defects in MLG compared to only 80 keV, as reported by Kim et al. (2008) and Girit et al. (2009). These results showed that MLG can achieve better radiation hardness as compared to commonly used Single or Bi-layer graphene.

Motivated by the better detection performance and radiation tolerance of thin-films Graphite as compared to Si, we further investigated the MLG performance as a detector material using Geant4. The detection performance was analyzed and discussed using the deposition energy, scattering angle, and detection efficiency resulting from the secondary particles in the interaction.

THE EFFECTS OF GRAPHENE THICKNESS AND KINETIC ENERGY OF THE INCIDENT ELECTRON ON THE DETECTION PROPERTIES OF GRAPHENE

Energy Deposition Analysis

Table 1 shows the effects of the thickness and incident

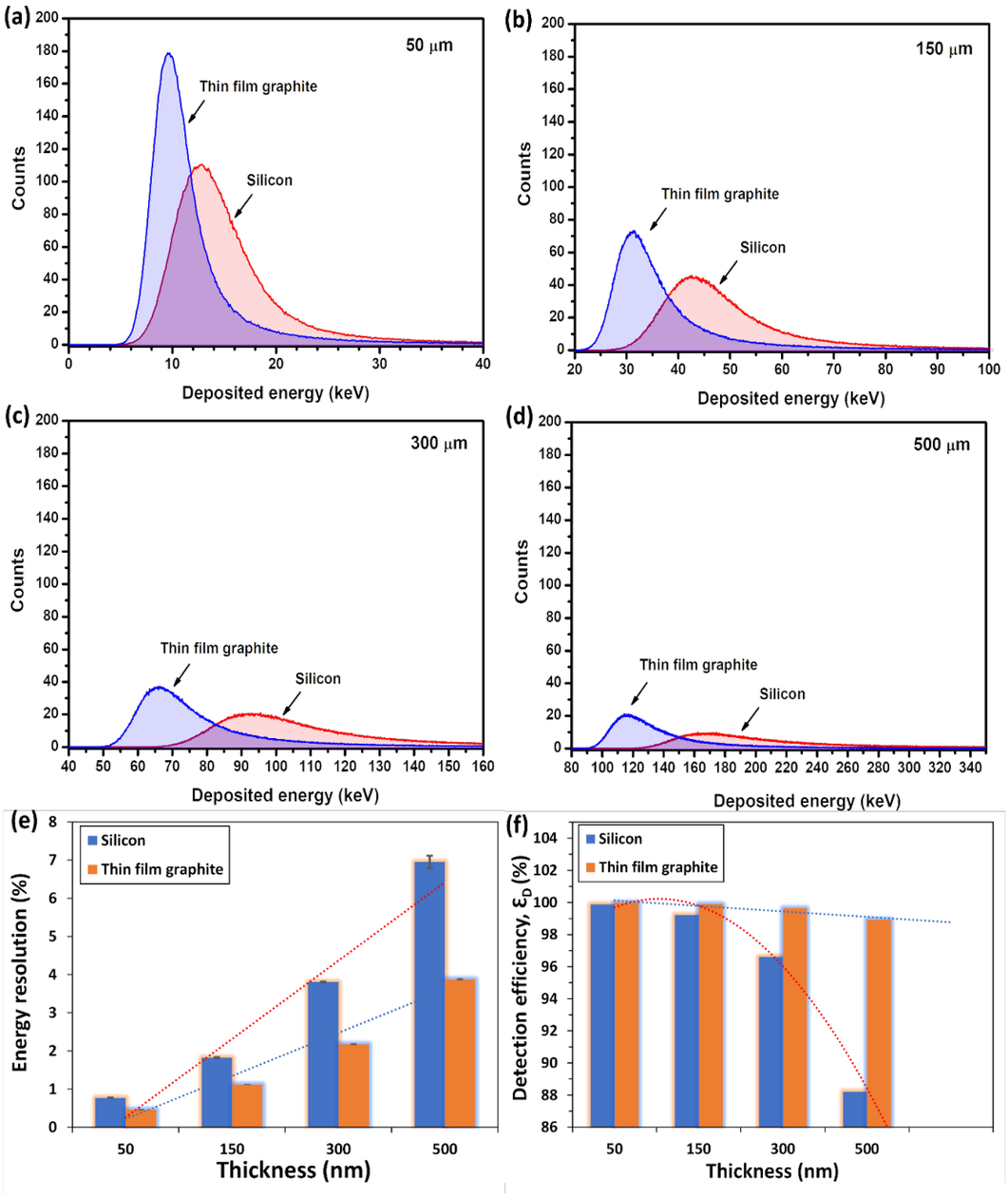

FIGURE 2. Energy spectra of deposited energy at (a) 50 μm, (b) 150 μm, (c) 300 μm, and (d) 500 μm thickness of Si and thin-films Graphite following interaction with 1 MeV electron. (e) Effect of Graphite thickness on energy resolution. (f) Effect of Graphite thickness on detection efficiency. Each bar represents mean ± standard deviation, with n = 1,000,000

electron energy on the deposited energy of MLG samples. The thicknesses of graphene layers in MLG varied from 3, 5, 10, 15, and 20 nm for each incident energy. Changes in the MLG thickness effectively modified the deposited energy in the interaction medium. The deposited energy significantly ($p<0.001$) increased with MLG thicknesses at all incident electron energies. Golunski and Postawa (2018) demonstrated that a much more significant

amount of deposited energy was obtained with a higher number of graphene layers, when bombarded with 5-40 keV of C60 ion. According to the Bethe Bloch formula with relativistic correction for interaction with electrons, the deposited energy was linearly dependent on the atomic number and the density of the interaction medium (Grupen et al. 2008; Le Bleis & Klenze 2014). The low atomic number of carbon atoms that made up the graphene and further reduction in the graphene thickness was attributed to the significant decrease in the deposited energy in the medium. However, the low atomic weight of carbon also resulted in a large cross-section when interacting with the electrons. It increased the possibilities of collision, which is essentially useful, especially for producing a highly sensitive medium for detector applications.

The incident electron energy also has a significant influence on the amount of deposited energy in the MLG. The significant reduction ($p<0.001$) in the amount of deposited energy was obtained with the medium and high-energy electron, while no significant reduction ($p>0.001$) was observed for very-high electron energies (E_{kin} > 100 MeV). This effect was due to the probability of energy loss from the incident particle being reduced with the increase of electron energy (Banhart et al. 2005; Zheng et al. 2015).

The higher amount of deposited energy obtained for the lower electron energy range originated from the ionization and multi scattering process which has become dominant for electron interactions within the range. The incident electron loses its energy from the secondary atomic electron's ejection during the process, known as delta-rays. Scattered electrons repeat the process until they leave the interaction medium (Khan & Gibbons 2010). The slower kinetic energy of the electron has a higher probability of interacting with a higher number of atomic electrons, and gets deposited with more energy during the interaction. These processes are reported to be the dominant contributor in energy loss for a charged particle with energy up to tens of MeV for electrons, before the radiative losses becomes dominant. Even though energy loss is small (typically tens of eV) for each interaction, the mean energy loss is still relatively high, since the cross-section is large. It can create defects that will affect the performance of the material (Lechner 2018). Instead of ionization, the interaction of the incident electron with the atomic nucleus also increases by slightly increasing the electron's kinetic energy to a few hundred keV. The high kinetic energy of the electron is needed for this kind of interaction to take place. Krasheninnikov and Banhart (2007) reported that a minimum energy of 100 keV is required to deposit approximately 20 eV of energy toward the carbon atoms. By increasing the kinetic energy to a very high energy range up to the GeV range, radiative losses from nuclear collisions becomes dominant (Tanabashi et al. 2018). However, this interaction is less frequent than the ionization interaction in the material. The incidence particle still loses some energy from the Coulomb interaction before additional losses from nuclear collision (Lechner 2018). Corresponding to the finite size of the nuclear target for interactions above tens of MeV, the mean energy losses from the coulombs scattering and non-ionizing energy losses approach a flattening phase with almost constant values, regardless of the medium thickness (Giani et al. 2014). Our results demonstrate a direct proportionality between the deposited energy and the thickness of graphene, and the effect of energy range on the interaction processes.

TABLE 1. Energy deposition in different thickness of MLG with variation of electron incident energy from 20 keV up to 1000 MeV

Thickness (nm)	Deposited energy (eV)							
	30 keV	50 keV	100 keV	500 keV	1 MeV	100 MeV	500 MeV	1000 MeV
3	4.371	2.991	1.863	0.9073	0.817	0.7924	0.7924	0.7924
5	7.287	4.986	3.106	1.512	1.362	1.321	1.321	1.321
10	14.67	9.973	6.212	3.024	2.723	2.641	2.641	2.641
15	21.98	15.06	9.32	4.537	4.085	3.962	3.962	3.962
20	29.21	20.07	12.44	6.049	5.446	5.282	5.283	5.283

Electron Beam Scattering

Table 2 shows the effects of thickness and incident electron energy on the scattering angles of the projected electrons following the interaction with MLG samples. The scattering angle increases significantly ($p<0.001$) with the MLG's thickness across all incident electron energies. A significant increase ($p<0.001$) in the scattering angle was also obtained with the increment of the electron energy from medium to high energy ranges ($30\ keV \leq E_{kin} \leq 100\ MeV$). Nonetheless, for the very-high energy range ($E_{kin} > 100\ MeV$), the reduction of the scattering angle was not significant ($p>0.001$) with the projected scattering angle approaching the initial incident of the electron beam's position. The larger scattering angles of electrons leaving the mediums indicate that more interactions occur with the atomic electron or carbon molecules in graphene. This result is consistent with the deposited energy, that shows a higher number of interactions appears with a thicker medium of interaction. It is inversely proportionate to the momentum of the incident particles. The minimal scattering angle is crucial for reducing particle attenuation, leading to misleading particle identification from tracking trajectory measurements, especially in high-energy environments. This result suggests that the MLG can be implemented as a detector material in a high-energy experiment which experiences a high fluence rate, and exposure to the radiation environment (Bachmair 2016). The minimal scattering angle in the MLG leads to a reduction in unwanted scattering, which helps in reducing the material budget from the additional structure and space required in detector construction (Kumar et al. 2018a, 2018b). This low material budget is favorable in high-energy experiments due to the limited space available within the detection area, and the limitation of the maintenance process inside the detection cavern (Schmidt 2016).

The correlations between the deposited energy and scattering angles of the MLG within the medium to the very high electron energy is shown in Figure 3. The result shows a positive linear correlation between both these parameters, with the Pearson correlation coefficient (R) calculated as 0.921 within all the sample thicknesses and energy ranges. This linear correlation implies that the scattering angle increases linearly with the increased deposition energy in the MLG. The deposited energy and scattering angles represent an important characteristic which affects the performance of the MLG as a detection material, specifically in high-energy environments. By understanding the correlation between both parameters, this can help to provide a better understanding of the performance of the MLG in different energy ranges. In 2013, Tielrooij et al. demonstrated the correlation between the photon energy levels, and the number of electron-electron scattering in graphene, following the typical carrier multiplication. The multiplication of electron cascades is related to the amount of materials available for interaction, which is the number of graphene layers in this study. A more significant number of interactions in the thicker medium, will result in a multiple scattering process from the longer projectile path, which increases the projected angle at the exit point of the medium (Golunski & Postawa 2018). Thus, the multiplication does not change the number of electrons available in the interaction medium, but results in a rise in the total amount of deposited energy following the interaction. The effect agrees with the present work that which shows a significant correlation between the deposited energy and scattering angles of the MLG in the different thicknesses and across the medium, to very-high electron incident energies.

TABLE 2. Scattering angle of projected electrons in different thickness of MLG with variation of electron incident energy from 20 keV up to 1000 MeV

Thickness (nm)	Scattering Angle (º)							
	30 keV	50 keV	100 keV	500 keV	1 MeV	100 MeV	500 MeV	1000 MeV
3	0.5006	0.3146	0.1693	0.0436	0.0248	0.0003	0.0001	0.0000
5	0.6607	0.4157	0.2240	0.0578	0.0330	0.0004	0.0001	0.0000
10	0.9604	0.6045	0.3260	0.0844	0.0481	0.0006	0.0001	0.0001
15	1.1924	0.7506	0.4052	0.1050	0.0599	0.0008	0.0002	0.0001
20	1.3901	0.8750	0.4728	0.1226	0.0700	0.0009	0.0002	0.0001

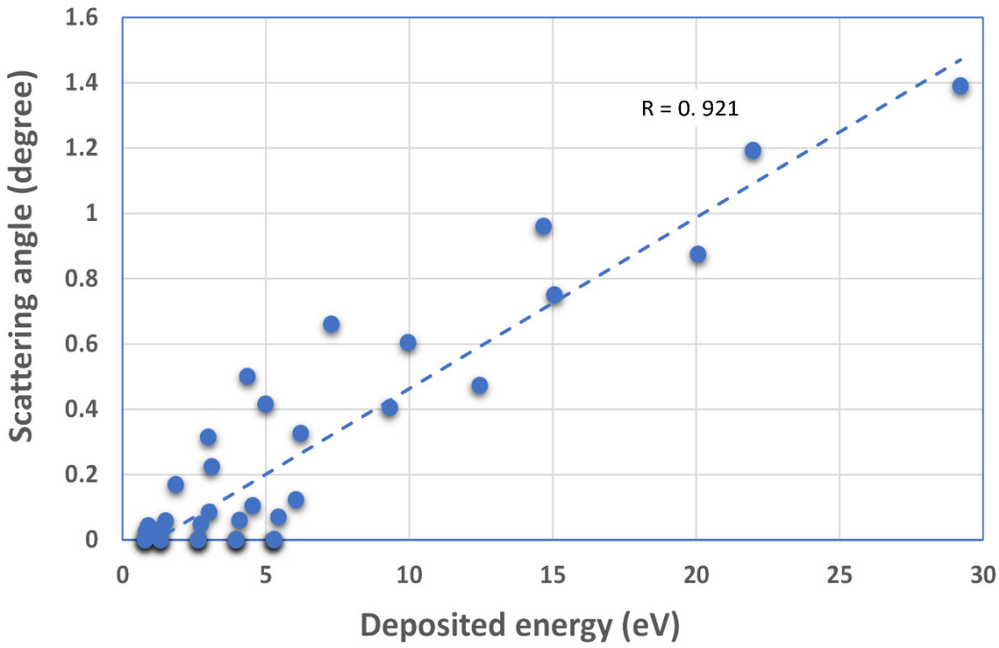

FIGURE 3. Correlation between deposited energy and scattering angle in MLG

Gamma Yield

Figure 4(a) & 4(b) shows the effects of electron incident energy on the gamma particle's yield from the interaction between the electron and MLG. This characteristic is used to measure the potential of the MLG as a detection material for solid-state photodetection applications in a high-energy environment. The gamma particles produced following each interaction are recorded as the gamma yield and calculated across the energy and corresponding thicknesses. The electron incident energy has a different influence on the yield of the gamma emitted following the interaction. The gamma yield decreases with the electron energy in the medium and high energy ranges (30 keV ≤ Ekin ≤ 100 MeV). The yield starts to saturate at E_{kin} > 500 keV, for all MLG thicknesses, with the highest reduction being observed for the 20 nm MLG. The gamma yield in this energy range originated from the inelastic scattering between the low-energy electrons and carbon shell electrons. The shell electrons which received energy from the incident electron are subsequently excited to higher energy states, and leave a vacancy in the orbital. The less tightly bound shell electrons from higher energy states will fill the vacancy, by releasing its energy through photon emission. The numbers increase depending on the intensities of the interaction which takes place. The highest yield of gamma was obtained in the 20 nm MLG, and reduces with the reduction of the MLG thickness. Furthermore, an increase in the electron's energy lowers the possibilities of interactions which occur in this thin film.

The correlations between the deposited energy and gamma yield of the MLG within the medium to high and very-high electron energy ranges are shown in Figure 4(c) & 4(d), respectively. The correlation coefficients were calculated to be 0.722 and 0.807, respectively, showing a positive linear correlation between both parameters. This linear correlation implies that the gamma yield increases linearly with the increase in the deposited energy in the MLG. The yield increased significantly ($p<0.001$) for very-high electron energies for all MLG thicknesses, due to the Bremsstrahlung process which became dominant in this energy range, and contributed to the rise in the gamma emission from the interaction (Lechner 2018). This significant increase was obtained for t> 10 nm, with the highest yield being observed in the 15 and 20 nm samples. The deceleration of the high-energy electrons in carbon was due to the Lorentz force from the atomic nucleus, which has been reported for critical energies of 81.7 MeV by Tanabashi et al. (2018). Berger et al. (1984) also reported on the critical energy of ~ 100 MeV for carbon atoms during the interaction with electrons. However, this Bremsstrahlung process became more intense with the increment of electron energies in the carbon atoms, compared to graphene,

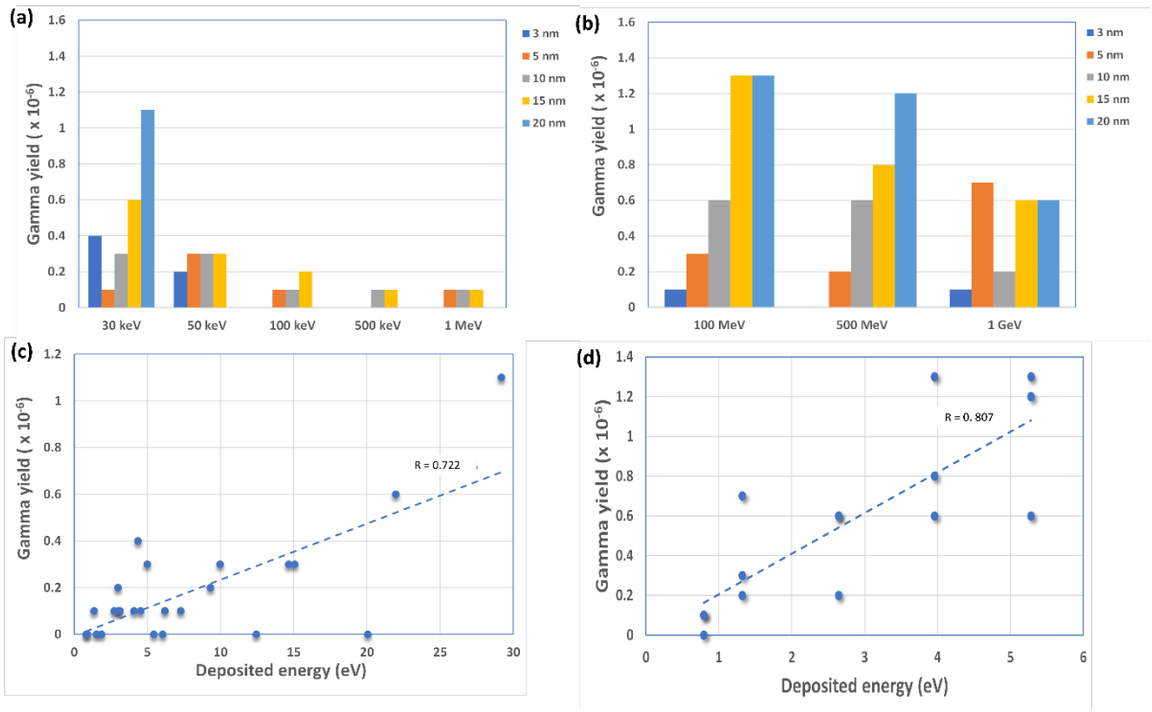

FIGURE 4. The yield of gamma particles created following the interaction with (a) Medium and (b) High electron energy range at different MLG thickness. Correlations between deposited energy and gamma yield following the interaction with (c) medium and (d) high electron energy range

which followed the reduction trends for energy larger than 500 MeV. The reduction of the gamma yield may also indicate the radiation blind properties of graphene at very-high energy ranges.

CONCLUSION

The studies were undertaken to compare the performance of Si and thin-films Graphite as detector materials, and have been presented in the first part of simulation results in this study. It was shown that the thin-films Graphite had a better performance in terms of signal generation, detection efficiency, and energy resolution, than Si under the high energy of 1 MeV electron irradiation. The energy resolution and detection efficiency of the thin-films Graphite showed further improvement with a lower t<150 nm thickness. Further studies on the multi-layer graphene with a much lower thickness in the nanometer range and electrical conductivity showed a degree of susceptibility for the material to signal generation under high-energy irradiation. Higher deposited energy was obtained with thicknesses >10 nm, indicating that the signal generation in the graphene was limited to the application of the 2D material in the detector application, which could be further improved using the graphene layering architecture. The low scattering angle of the MLG for high energy ranges (E_{kin}> 1 MeV), regardless of the thickness, proved that further reduction of the material budget in the detector could be achieved. A low particle attenuation was obtained for (E_{kin}> 500 keV), which suggested better detection efficiencies for the MLG, which can be achieved using this material. The results obtained from this study have provided a better understanding of the performance of graphene MLGs under various incident kinetic energy electron beam irradiation. It suggests that MLGs could be a potential candidate as a detection material for future application in HEP experiments. For future work, it is recommended that the defects created by the high-energy irradiation in graphene layers are further investigated.

ACKNOWLEDGEMENTS

Author Nurul Hidayah Mohamad Nor would like to acknowledge the Ministry of Higher Education (MOHE), Malaysia and University Malaya (UM), for the scholarship support (HLCB).

REFERENCES

Ang, P.K., Chen, W., Wee, A.T.S. & Kian, P.L. 2008. Solution-gated epitaxial graphene as pH sensor. *Journal of the American Chemical Society* 130(44): 14392-14393. doi:10.1021/ja805090z.

Bachmair, F. 2016. CVD diamond sensors in detectors for high energy physics. PhD Thesis. ETH Zürich (Unpublished). https://doi.org/10.3929/ethz-a-010748643.

Balandin, A.A. 2011. Thermal properties of graphene and nanostructured carbon materials. *Nature Materials* 10(8): 569-581. doi:10.1038/nmat3064.

Banhart, F. 1999. Irradiation effects in carbon nanostructures. *Reports on Progress in Physics* 62(8): 1181-1221. doi:10.1088/0034-4885/62/8/201.

Banhart, F., Li, J.X. & Krasheninnikov, A.V. 2005. Carbon nanotubes under electron irradiation: Stability of the tubes and their action as pipes for atom transport. *Physical Review B - Condensed Matter and Materials Physics* 71(24): 1-4. doi:10.1103/PhysRevB.71.241408.

Berger, M.J., Inokuti, M., Anderson, H.H., Bichsel, H., Dennis, J.A., Powers, D., Seltzer, S.M. & Turner, J.E. 1984. Stopping powers for electrons and positrons. *Journal of the International Commission on Radiation Units and Measurements* 19(2): 281. doi:https://doi.org/10.1093/jicru/os19.2.Report37.

Biswas, S. & Drzal, L.T. 2010. Multilayered nano-architecture of variable sized graphene nanosheets for enhanced supercapacitor electrode performance. *ACS Applied Materials and Interfaces* 2(8): 2293-2300. doi:10.1021/am100343a.

Bortoletto, D. 2015. How and why silicon sensors are becoming more and more intelligent? *Journal of Instrumentation* 10(8). doi:10.1088/1748-0221/10/08/C08016.

Buckley, A., Krauss, F., Plätzer, S., Seymour, M., Alioli, S., Andersen, J., Bellm, J., Butterworth, J., Dasgupta, M., Duhr, C., Frixione, S., Gieseke, S., Hamilton, K., Hesketh, G., Hoeche, S., Jung, H., Kilian, W., Lönnblad, L., Maltoni, F., Mangano, M., Mrenna, S., Nagy, Z., Nason, P., Nurse, E., Ohl, T., Oleari, C., Papaefstathiou, A., Plehn, T., Prestel, S., Ré, E., Reuter, J., Richardson, P., Salam, G., Schoenherr, M., Schumann, S., Siegert, F., Siódmok, A., Sjödahl, M., Sjöstrand, T., Skands, P., Soper, D., Soyez, G. & Webber, B. 2019. Monte Carlo event generators for high energy particle physics event simulation. *arXiv*. https://arxiv.org/abs/1902.01674

Carrier, J.F., Archambault, L., Beaulieu, L. & Roy, R. 2004. Validation of GEANT4, an object-oriented Monte Carlo toolkit, for simulations in medical physics. *Medical Physics* 31(3): 484-492. doi:10.1118/1.1644532.

Castro Neto, A.H., Guinea, F., Peres, N.M.R., Novoselov, K.S. & Geim, A.K. 2009. The electronic properties of graphene. *Reviews of Modern Physics* 81(1): 109-162. doi:10.1103/RevModPhys.81.109.

Compagnini, G., Giannazzo, F., Sonde, S., Raineri, V. & Rimini, E. 2009. Ion irradiation and defect formation in single layer graphene. *Carbon* 47(14): 3201-3207. doi:10.1016/j.carbon.2009.07.033.

Demir, N. & Kuluöztürk, Z.N. 2021. Determination of energy resolution for a NaI(Tl) detector modeled with FLUKA code. *Nuclear Engineering and Technology* 53(11): 3759-3763. doi:10.1016/J.NET.2021.05.017.

Giani, S., Leroy, C., Price, L., Rancoita, P-G. & Ruchti, R. 2014. Astroparticle, particle, space physics and detectors for physics applications. *Astroparticle, Particle, Space Physics, Radiation Interaction, Detectors and Medical Physics Applications*. *Vol. 8.* doi:doi:10.1142/9166.

Girit, Ç.Ö., Meyer, J.C., Erni, R., Rossell, M.D., Kisielowski, C., Yang, L., Park, C.H., Crommie, M.F., Cohen, M.L., Louie, S.G. & Zettl, A. 2009. Graphene at the edge: Stability and dynamics. *Science* 323(5922): 1705-1708. doi:10.1126/science.1166999.

Golunski, M. & Postawa, Z. 2018. Effect of kinetic energy and impact angle on carbon ejection from a free-standing graphene bombarded by kilo-electron-volt C 60. *Journal of Vacuum Science & Technology B, Nanotechnology and Microelectronics: Materials, Processing, Measurement, and Phenomena* 36(3): 03F112. doi:10.1116/1.5019732.

Grupen, C., Shwartz, B.A. & Spieler, H. 2008. *Particle Detectors*. Cambridge: Cambridge University Press.

Guatelli, S., Cutajar, D., Oborn, B. & Rosenfeld, A.B. 2011. Introduction to the geant4 simulation toolkit. *AIP Conference Proceedings* 1345: 303-322. doi:10.1063/1.3576174.

Hartmann, F. & Kaminski, J. 2011. Advances in tracking detectors. *Annual Review of Nuclear and Particle Science* 61: 197-221. doi:10.1146/annurev-nucl-102010-130052.

Holbert, K.E. 2012. Charged particle ionization and range. *EEE460-Handout*.

Hossain, I., Sharip, N. & Viswanathan, K.K. 2012. Efficiency and resolution of HPGe and NaI(Tl) detectors using gamma-ray spectroscopy. *Scientific Research and Essays* 7(1): 86-89. doi:10.5897/sre11.1717.

Jeong, H.Y., Lee, D-S., Choi, H.K., Lee, D.H., Kim, J-E., Jeong, H.Y., Lee, D-S., Choi, H.K., Lee, D.H. & Kim, J-E. 2010. Flexible room-temperature NO_2 gas sensors based on carbon nanotubes/reduced graphene hybrid films flexible room-temperature NO_2 gas sensors based on carbon nanotubes/reduced graphene hybrid films. *Applied Physics Letters* 96: 213105. doi:10.1063/1.3432446.

Khan, F.M. & Gibbons, J.P. 2010. *The Physics of Radiation Therapy*. 5th ed. Philadelphia: Wolters Kluwer.

Kholili, J. 2015. Using graphene as ion detector. Master Thesis. Chalmers University of Technology, Gothenburg Sweden (Unpublished).

Kim, K.J., Choi, J., Lee, H., Lee, H.K., Kang, T.H., Han, Y.H., Lee, B.C., Kim, S. & Kim, B. 2008. Effects of 1 MeV electron beam irradiation on multilayer graphene grown on 6H-SiC(001). *Journal of Physical Chemistry C* 112(34): 13062-13064. doi:10.1021/jp805141e.

Krasheninnikov, A.V. & Banhart, F. 2007. Engineering of nanostructured carbon materials with electron or ion beams. *Nature Mate* 6: 723-733. doi:10.1038/nmat1996.

Kumar, S., Reshi, B.A. & Varma, R. 2018a. Comparison of silicon, germanium, gallium nitride, and diamond for using as a detector material in experimental high energy physics. *Results in Physics* 11(August): 461-474. doi:10.1016/j.rinp.2018.08.045.

Kumar, S., Varma, R., Das Gupta, K., Sarin, P. & Deb, S.K. 2018b. Comparison of Si, Ge, and diamond sensors for using it in hep experiments. *Springer Proceedings in Physics* 201: 97-105. doi:10.1007/978-981-10-7665-7_9.

Le Bleis, T. & Klenze, P. 2014. Physics simulation with Geant4. *Technical University Munich*. https://www.ph.tum.de/academics/org/labs/fopra/docs/userguide-77.en.pdf

Lechner, A. 2018. Particle interactions with matter. *CERN Yellow Reports: School Proceedings* 5(March): 47-68. doi:10.23730/CYRSP-2018-005.47.

Lee, C., Wei, X., Kysar, J.W. & Hone, J. 2008. Measurement of the elastic properties and intrinsic strength of monolayer graphene. *Science* 321(5887): 385-388. doi:10.1126/science.1156211.

Lin, Y-M., Jenkins, K.A., Valdes-garcia, A., Small, J.P., Farmer, D.B. & Avouris, P. 2009. Operation of graphene transistors at gigahertz frequencies. *Nano Letters* 9(1): 422-426. doi:10.1021/nl803316h.

Liu, H., Liu, Y. & Zhu, D. 2011. Chemical doping of graphene. *Journal of Materials Chemistry* 21(10): 3335-3345. doi:10.1039/c0jm02922j.

Lu, G., Ocola, L.E. & Chen, J. 2009. Reduced graphene oxide for room-temperature gas sensors. *Nanotechnology* 20(44): 445502. doi:10.1088/0957-4484/20/44/445502.

Mayorov, A.S., Gorbachev, R.V., Morozov, S.V., Britnell, L., Jalil, R., Ponomarenko, L.A., Blake, P., Novoselov, K.S., Watanabe, K., Taniguchi, T. & Geim, A.K. 2011. Micrometer-scale ballistic transport in encapsulated graphene at room temperature. *Nano Letters* 11(6): 2396-2399. doi:10.1021/nl200758b.

Meroli, S. 2015. *Interaction of Radiation with Matter: From the Theory to the Measurements*. https://www.researchgate.net/publication/283855144_Interaction_of_radiation_with_matter_from_the_theory_to_the_measurements

Metcalfe, J., Mejia, I., Murphy, J., Quevedo, M., Smith, L., Alvarado, J., Gnade, B. & Takai, H. 2014. Potential of thin films for use in charged particle tracking detectors. http://arxiv.org/abs/1411.1794.

Meyer, J.C., Kisielowski, C., Erni, R., Rossell, M.D., Crommie, M.F. & Zettl, A. 2008. Direct imaging of lattice atoms and topological defects in graphene membranes. *Nano Letters* 8(11): 3582-3586. doi:10.1021/nl801386m.

Moll, M. 2006. Radiation tolerant semiconductor sensors for tracking detectors. *Nuclear Instruments and Methods in Physics Research, Section A: Accelerators, Spectrometers, Detectors and Associated Equipment* 565(1): 202-211. doi:10.1016/j.nima.2006.05.001.

Moser, J., Barreiro, A. & Bachtold, A. 2007. Current-induced cleaning of graphene. *Applied Physics Letters* 91(16): 1-4. doi:10.1063/1.2789673.

Murata, H., Nakajima, Y., Saitoh, N., Yoshizawa, N., Suemasu, T. & Toko, K. 2019. High-electrical-conductivity multilayer graphene formed by layer exchange with controlled thickness and interlayer. *Scientific Reports* 9(1): 1-5. doi:10.1038/s41598-019-40547-0.

Nur Afira binti Anuar, Nurul Hidayah Mohamad Nor, Rozidawati binti Awang, Hideki Nakajima, Sarayut Tunmee, Manoj Tripathi, Alan Dalton & Boon Tong Goh. 2021. Low-temperature growth of graphene nanoplatelets by hot-wire chemical vapour deposition. *Surface and Coatings Technology* 411: 126995. doi:10.1016/j.surfcoat.2021.126995.

Razaghi, S., Saramad, S. & Shamsaei, M. 2019. Simulation study of resistive plate chamber's (RPCs) capability for medical imaging applications. *Journal of Instrumentation* 14: P01024.

Robinson, J.T., Keith Perkins, F., Snow, E.S., Wei, Z. & Sheehan, P.E. 2008. Reduced graphene oxide molecular sensors. *Nano Letters* 8(10): 3137-3140. doi:10.1021/nl8013007.

Schedin, F., Geim, A.K., Morozov, S.V., Hill, E.W., Blake, P., Katsnelson, M.I. & Novoselov, K.S. 2007. Detection of individual gas molecules adsorbed on graphene. *Nature Materials* 6(9): 652-655. doi:10.1038/nmat1967.

Schmidt, B. 2016. The high-luminosity upgrade of the LHC: Physics the high-luminosity upgrade of the LHC physics and technology challenges for the accelerator and the experiments. *Journal of Physics: Conference Series* 706: 22002. doi:10.1088/1742-6596/706/2/022002.

Singh, V., Joung, D., Zhai, L., Das, S., Khondaker, S.I. & Seal, S. 2011. Graphene based materials: Past, present and future. *Progress in Materials Science* 56(8): 1178-1271. doi:10.1016/j.pmatsci.2011.03.003.

Spieler, H. 2005. *Semiconductor Detector Systems*. Oxford: Clarendon Press.

Tanabashi, M., Hagiwara, K., Hikasa, K., Nakamura, K., Sumino, Y., Takahashi, F., Tanaka, J., et al. 2018. Review of particle physics. *Physical Review D* 98(3): 30001. doi:10.1103/PhysRevD.98.030001.

Tielrooij, K.J., Song, J.C.W., Jensen, S.A., Centeno, A., Pesquera, A., Zurutuza Elorza, A., Bonn, M., Levitov, L.S. & Koppens, F.H.L. 2013. Photoexcitation cascade and multiple hot-carrier generation in graphene. *Nature Physics* 9(4): 248-252. doi:10.1038/nphys2564.

Wang, J., Chen, D., Chen, T. & Shao, L. 2020. Displacement of carbon atoms in few-layer graphene. *Journal of Applied Physics* 128: 085902. doi:10.1063/5.0013310.

Zhang, T., Cheng, Z., Wang, Y., Li, Z., Wang, C., Li, Y. & Fang, Y. 2010. Self-assembled 1-octadecanethiol monolayers on graphene for mercury detection. *Nano Letters* 10(11): 4738-4741. doi:10.1021/nl1032556.

Zheng, X., Chen, W., Wang, G., Yu, Y., Qin, S., Fang, J., Wang, F. & Zhang, X.A. 2015. The Raman redshift of graphene impacted by gold nanoparticles. *AIP Advances* 5(5): 1-8. doi:10.1063/1.4921316.

*Corresponding author; email: nurulhidayah@um.edu.my